2015

Functional Properties of APCVD VO2 Layers

Dimitra Vernardou
Center of Materials Technology and Photonics, School of Applied Technology, Technological Educational Institute of Crete, 710 04 Heraklion, Crete, Greece., dimitra@iesl.forth.gr

Dimitrios Louloudakis
Center of Materials Technology and Photonics, School of Applied Technology, Technological Educational Institute of Crete, 710 04 Heraklion, Crete, Greece\\ Department of Physics, University of Crete, 710 03 Heraklion, Crete, Greece, dimitr17@yahoo.gr

Emmanuel Spanakis
Department of Materials Science and Technology, University of Crete, 710 03 Heraklion, Crete, Greece, spanakis@materials.uoc.gr

Nikolaos Katsarakis
Center of Materials Technology and Photonics, School of Applied Technology, Technological Educational Institute of Crete, 710 04 Heraklion, Crete, Greece. \\ Electrical Engineering Department, School of Applied Technology, Technological Educational Institute of Crete, 710 04 Heraklion, Crete, Greece. \\ Institute of Electronic Structure and Laser, Foundation for Research & Technology- Hellas, P.O. Box 1527, Vassilika Vouton, 711 10 Heraklion, Crete, Greece, katsan@iesl.forth.gr

Emmanuel Koudoumas
Center of Materials Technology and Photonics, School of Applied Technology, Technological Educational Institute of Crete, 710 04 Heraklion, Crete, Greece. \\ Institute of Electronic Structure and Laser, Foundation for Research & Technology- Hellas, P.O. Box 1527, Vassilika Vouton, 711 10 Heraklion, Crete, Greece, koudoumas@staff.teicrete.gr

Int. J. Thin. Fil. Sci. Tec. **4**, No. 3, 187-191 (2015)

187

Functional Properties of APCVD VO₂ Layers

D. Vernardou[*,1], *D. Louloudakis*[*1,2], *E. Spanakis*[3], *N. Katsarakis*[1,4,5] and *E. Koudoumas*[1,5].

[1]Center of Materials Technology and Photonics, School of Applied Technology, Technological Educational Institute of Crete, 710 04 Heraklion, Crete, Greece.

[2]Department of Physics, University of Crete, 710 03Heraklion, Crete, Greece.

[3]Department of Materials Science and Technology, University of Crete, 710 03, Heraklion, Crete, Greece.

[4]Electrical Engineering Department, School of Applied Technology, Technological Educational Institute of Crete, 710 04 Heraklion, Crete, Greece.

[5]Institute of Electronic Structure and Laser, Foundation for Research & Technology-Hellas, P.O. Box 1527, Vassilika Vouton, 711 10 Heraklion, Crete, Greece.

Abstract: The growth of isolated monoclinic and metastable vanadium dioxide phases was possible by the atmospheric pressure chemical vapor deposition at 500 ºC through the control of oxygen flow rate. The as-grown coating for 0.2 L min^{-1} showed a reversible switching behavior at 62 ºC with a difference in transmittance of the order of 40 %. On the other hand, the coating deposited for 0.8 L min^{-1} had good electrochemical response presenting capacitance retention of 96 % after 500 scans. The results are discussed in terms of the materials' observed structure and morphology. We showed that the transition characteristics of the coatings are based on the competing effects of crystallinity and crystallite size, while their electrochemical response is related to the increased surface area ratio of the nanorods.

Keywords: APCVD, VO₂, Thermochromics, Capacitors.

1 Introduction

Vanadium dioxide (VO_2) is a material of interest because it undergoes a reversible metal-semiconductor phase transition at 68 ºC [1]. The transition is associated with a structural change from a low temperature semiconducting monoclinic phase (VO_2 (M)) to a high temperature metallic rutile phase (VO_2 (R)) [2, 3]. The monoclinic phase is transmissive to a wide range of solar radiation, while the rutile phase is reflective to solar radiation especially that in the infrared region [4]. These characteristics make VO_2 coatings suitable for optical switches [5], modulators [6], optical data storage medium [7] and thermochromic windows [8-10]. Additionally, there is a particular interest in the metastable VO_2 (VO_2 (B)) as a cathode material in lithium ion batteries (LIBs) because it can deliver a high amount of lithium storage [11, 12] owing to its layered structure consisting of distorted VO_6 octahedra [13].

There have been numerous studies of the chemical vapor deposition at atmospheric pressure (APCVD) of VO_2 including the reaction of vanadium (IV) chloride (VCl_4) with water in a cold-wall horizontal reactor [14]. Vanadium (V) oxytrichloride ($VOCl_3$) has also been used with water at temperatures higher than 600 ºC [15]. In this case, mixed

phase of V_2O_5 and V_6O_{13} were produced, which were reduced by controlling the flow rates through the reactor. Maruyama and Ikuta have utilized vanadyl (III) acetylacetonate ($V(acac)_3$) as a single-source precursor through a slow post-deposition cooling process [16]. Other vanadyl compounds for the preparation of VO_2 were the vanadyl (IV) acetylacetonate ($VO(acac)_2$) [17] and vanadium (V) triisopropoxide ($VO(OC_3H_7)_3$) [18-20].

The process has fast deposition rates and the advantage of being easily integrated into float-glass production lines. In addition, the stoichiometry, thickness and morphological characteristics of the coatings can be controlled through the growth temperature and time, precursors utilized, N_2 flow rate through the reactor, substrate etc. However, one of the challenges for the APCVD approach is a place in the so-called roll-to-roll industrial processing methods since they are regarded as inexpensive, high speed and high volume manufacturing. Hence, our interest was directed towards the growth of VO_2 on flexible substrates, which are light weight and transparent and could potentially be used in window and other applications.

This paper reports the APCVD of VO_2 layers using $VO(acac)_2$ as vanadium precursor on flexible substrates. On controlling the oxygen flow rate, isolated monoclinic and

*Corresponding author E-mail: dimitra@iesl.forth.gr

metastable VO_2 nanocrystallites and nanorods were obtained, respectively. It will be shown that the hysteresis width and the difference in transmittance between the metallic and the semiconducting phase increase due to the enhancement of crystallinity and crystallite size in VO_2 (M) layers. Finally, only the VO_2 (B) presented electrochemical response, which was inverted and repeatable with minimal degradation at least for 500 scans presenting a discharge capacity of 189 mAh g^{-1}.

2 Experimental

The APCVD reactor used in this work was also reported previously [21, 22]. The vanadium precursor was the $VO(acac)_2$ (98 %, Sigma-Aldrich), which was placed in a bubbler at 200 ºC, while the gas lines were kept at 220 ºC to enhance transport of precursor and to prevent condensation in the lines. The carrier gas was nitrogen (99.9 %), which was passed through the apparatus during all operations of the reactor. The growth temperature and time were 500 ºC and 30 min for all coatings. The amount of oxygen added (flow rate), which acted as oxidant during the CVD processes was 0, 0.2, 0.4 and 0.8 L min^{-1}. Finally, the nitrogen flow rate passing through the vanadium bubbler was kept at 1.4 L min^{-1}, while the total flow rate in all experiments was 12 L min^{-1}. The substrates were flexible corning® willow® glass, all of dimensions 2 cm x 2 cm x 200 μm. Prior to deposition, all substrates were cleaned with H_2O and detergent, rinsed thoroughly with H_2O and deionised H_2O and allowed to dry in air.

X-ray diffraction (XRD) measurements were carried out in a Siemens D5000 Diffractometer for 2-theta = 20.00-30.00 º, step size 0.05 º and step time 5 min/º. The morphology of the samples was studied using a Jeol JSM-7000F field-emission scanning electron microscope (FE-SEM). Samples were over-coated with a thin film of gold prior to analysis to prevent charging. The transmittance measurements were performed in a Perkin Elmer Lambda 950 spectrophotometer over the wavelength range of 250-2500 nm at 25 and 90 ºC, while the transmittance-temperature studies were done using a tungsten-halogen lamp at 1500 ± 20 nm. Additionally, cyclic voltammetry experiments were performed using a three electrode electrochemical cell [23-26] and a computer-controlled AUTOLAB potentiostat/galvanostat. Ag/AgCl and Pt foil were employed as the reference and the counter electrodes, respectively. Vanadium oxides coatings on flexible glass substrates were acted as the working electrodes biased in the range between -2 V and +2 V. The measurements were performed in 1 M, aqueous $LiClO_4$ for a scan rate of 10 mV s^{-1} and scanned up to 500 times. The chronopotentiometric tests were carried out at a current density of 1 A g^{-1} for a period of 500 s.

3 Results and Discussion

In these experiments, growth temperatures higher than 450 ºC were necessary for the formation of VO_2 layers, which reflects the intramolecular decomposition mechanism expected for $VO(acac)_2$ [21]. The coatings were stable in air for over six months presenting similar structural, morphological and thermochromic properties. In addition, they were resistant to common solvents such as H_2O and acetone.

Figure 1 shows the XRD patterns for the as-grown coatings using oxygen flow rates of 0, 0.2, 0.4 and 0.8 L min^{-1}, which are maximized in the short range of 20-30 º to enhance the peaks signal. The addition of oxygen is necessary to induce the growth of VO_2 coatings, since only a broad background is observed from 20 to 27 º due to the underlying substrate for 0 L min^{-1}. It is worth noting that for oxygen flow rates of 0.2 and 0.8 L min^{-1}, the formation of single-phase monoclinic [14] (27.8 º) and metastable [27] (28.3 º) VO_2 coatings, respectively is predominant. On the other hand, for oxygen flow rate of 0.4 L min^{-1} at the same growth temperature as before, both VO_2 phases are present.
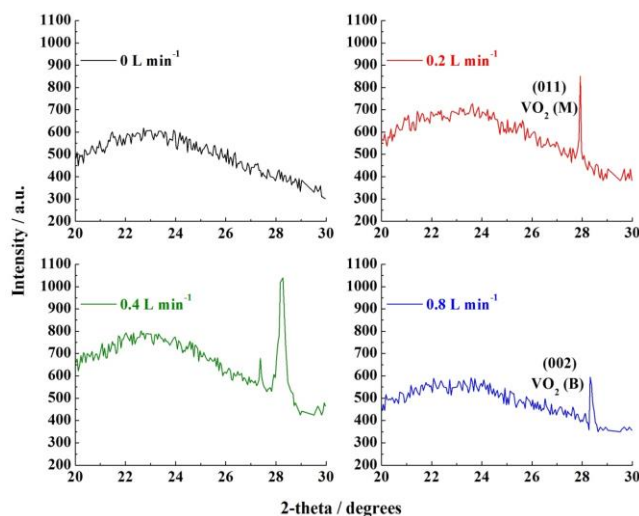

Fig. 1. XRD of APCVD vanadium oxide at 500 ºC using oxygen flow rate of 0, 0.2, 0.4 and 0.8 L min^{-1}.

FE-SEM images suggest the formation of nanocrystallites of ca. 200-400 nm in width for the monoclinic VO_2 (0.2 L min^{-1}) and nanorods of 300-400 nm in thickness and 20-30 nm in width for the metastable VO_2 phase (0.8 L min^{-1}) as shown in Figures 2 (b) and (d). On the other hand, both structures are present for the as-grown coating at 0.4 L min^{-1} (Figure 2 (c)). This observation along with the XRD patterns clearly indicates the possibility to isolate the two VO_2 phases depending on the oxygen flow rate utilized. Finally, the coating grown for 0 L min^{-1} consists of a thin layer that appears to be free of crystallite boundaries.

From the deposition time and coating thickness as determined by the cross-section of the FE-SEM images (Figure 2 (a)-(d) insets), effective deposition rates were obtained with a maximum value being at 0.8 L min^{-1} (15.7 ± 5 nm min^{-1}). Below 0.8 L min^{-1}, the rate falls off from 8.6 ± 4 (0.2 L min^{-1}) to 7 ± 3 nm min^{-1} (0.4 L min^{-1}). The fall-off in growth rate at 0.4 L min^{-1} can be attributed to either

coating decomposition [28] or pathways, which reduce precursor concentrations [29]. Since coating decomposition does not occur for this system, it is suggested that at this flow rate, the precursor pre-reacts with oxygen in the gas phase. However, taking into consideration the approximation in deposition rate's estimation, it may also be the case that there is a window in the flow-rate-control regime of the growth process where growth occurs independently of oxygen flow rate. This seems to be unlikely in view of the morphological changes noted, which clearly demonstrate that changing oxygen flow rate has a significant effect upon the nature of the growing coatings as shown in Figure 2.
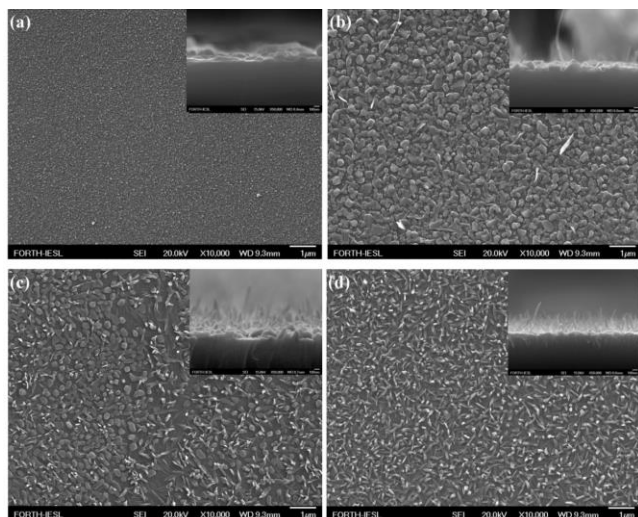

Fig. 2. FE-SEM images of APCVD vanadium oxide at 500 ºC using oxygen flow rate of 0 (a), 0.2 (b), 0.4 (c) and 0.8 L min^{-1} (d). Cross-sections with a magnification of x50, 000 are also indicated as insets

A proposed mechanism for the formation and growth process of the transformation from nanocrystallites VO_2 (M) to nanorods VO_2 (B) can be the following: At the initial stage, in the absence of oxygen, crystallites free of regions were nucleated and grew further as the oxygen flow rate increased to 0.2 L min^{-1}. Some of them were stacked on the top of each other forming the base of the nanorods at 0.4 L min^{-1} resulting in both monoclinic and metastable VO_2. Finally, the nanorods were completely formed at 0.8 L min^{-1} and VO_2 (B) phase was obtained. On the basis of the above results, the whole evolution of VO_2 (M) nanocrystallites to VO_2 (B) nanorods is illustrated in Figure 3.
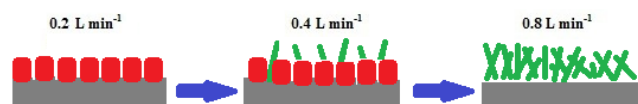

Fig. 3. Growth of nanocrystallites VO_2 (M) to nanorods VO_2 (B). Red and green colors refer to VO2 (M) and VO2 (B), respectively.

The transition temperature (T_c), hysteresis width and difference in transmittance (ΔT) between the metallic and the semiconducting phase of these coatings were studied through the change in transmittance at 1500 nm as shown in

Figure 4. Those grown for 0 and 0.8 L min^{-1} did not present thermochromic behavior due to the lack of oxide formation and the presence of VO_2 (B) [30], respectively. From the parameters estimated, the coating grown for 0.2 L min^{-1} presented the highest difference in transmittance (ΔT), being 40 % (15 % for 0.4 L min^{-1}) and the lowest T_c of 62 ºC (67 ºC for 0.4 L min^{-1}). On the other hand, the hysteresis width was narrower for the 0.4 L min^{-1}, being 10 ºC in contrast with the 0.2 L min^{-1}, which found to be 21 ºC. The hysteresis width estimated for 0.2 L min^{-1} is similar with the APCVD of VO_2 coatings using VCl_4 at 550 ºC [31] and $VO(acac)_2$ at 600 ºC [32]. Additionally, a large change in transmittance between the two phases has been observed by an APCVD system (i.e. 50 %) using $VO(acac)_2$ as in this work, but with the addition of tungsten dopant [31].
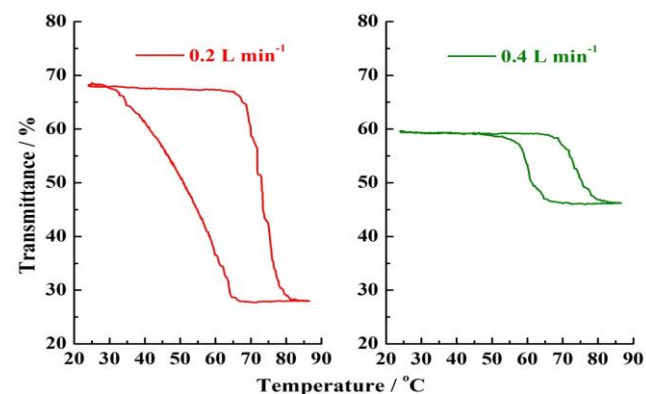

Fig. 4. Transmittance at 1500 nm against temperature for the as-grown vanadium oxides using oxygen flow rate of 0.2 and 0.4 L min^{-1}

Generally, the different phase transition properties of the VO_2 coatings can be attributed to structural defects, film stoichiometry and internal stress [33-36].
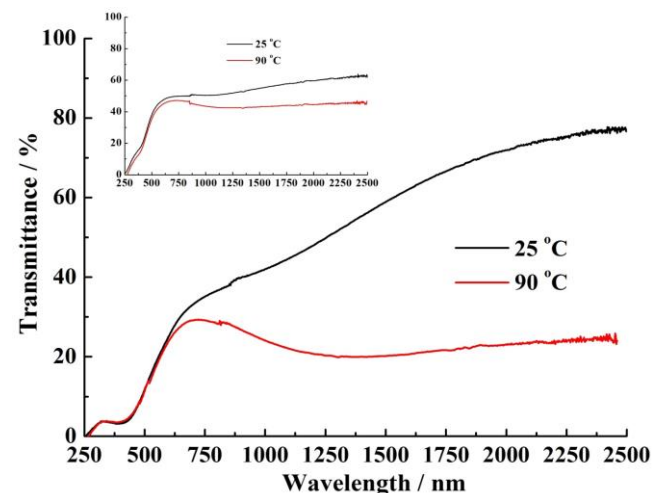

Fig. 5. Transmittance spectra below T_c at 25 and above T_c at 90 ºC over the region of 250 – 2500 nm for the vanadium oxide coatings grown using oxygen flow rate of 0.2 and 0.4 L min^{-1} (inset).

For instance, Kang et. al. investigated the hysteresis width of VO_2 coatings and found a broader width for those with

smaller particles due to the larger interfacial energies and the lack of defects for nucleation [37]. Additionally, Klimov et. al. suggested through a model that the hysteresis width decreases with increasing the particle size [38]. However, the opposite behavior has been observed for our samples. As the crystallites are smaller in size for the higher oxygen flow rates, the hysteresis width gets narrower. This contradiction can be explained by the hypothesis that the metal-semiconductor phase transition in VO_2 can be described through the model of a martensitic transformation in which the structural defects play the essential role in the phase transformation [39, 40]. As the oxygen flow rate increases, the number of those defects that can give rise to the phase transition is increased; this is supported by the decreasing width of the VO_2 (M) peak in XRD with the simultaneous enhancement of the one for VO_2 (B). Therefore, the hysteresis width narrows in the coatings with the smaller crystallites because the phase transition can easily occur in this defective structure. Moreover, the crystallite boundaries can also be thought to be a source of nucleating defects that diminish with larger crystallite size [41].
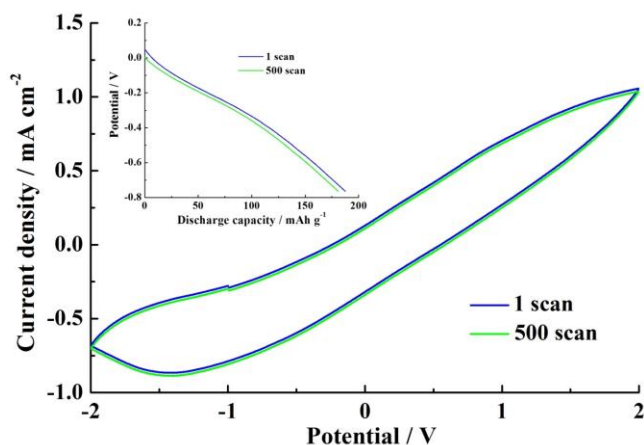

Fig. 6. Cyclic voltammograms of the first and the 500th scan for the as-grown VO2 (B) coating using a scan rate of 10 mV s-1 and an electrode active area of 1 cm2. Chonopotentiometric curves of the same sample at 1 A g-1 as inset.

One may then suggest that the enhancement of VO_2 (M), which accompanies the crystallite growth results in larger hysteresis width, as there are fewer nucleating defects. The hysteresis cycle is thus determined by the competing effects of crystallinity and crystallite size. Finally, the magnitude of the metal-semiconductor phase transition, being the highest for 0.2 L min^{-1} as implied by the 40 % change of transmittance, seems to be more sensitive to the presence of single-phase VO_2 (M) [42].

The thermally induced, reversible, metal-to-semiconductor transition of the coatings grown for oxygen flow rate of 0.2 and 0.4 L min^{-1} is shown in Figure 5. Both coatings display properties required for thermochromic applications, i.e. decrease in NIR region with little change in the visible region. These measurements were repeated after six months and found to be exactly the same.

In order to study the electrochemical stability of the coatings, cyclic voltammetric curves were obtained sweeping the potential from -2 V to +2 V and back for a scan rate of 10 mV s^{-1}. The metastable VO_2 coating exhibits one cathodic and one anodic peak at approximately -1.5 V, which are attributed to Li$^+$ intercalation and deintercalation, respectively as shown in Figure 6. Furthermore, no significant long-terms degradation can be observed as evident from the similarity between the 1st (blue) and 500th (green) scan indicating a good electrochemical stability. On the other hand, the samples grown for 0.2 and 0.4 L min^{-1} oxygen flow rate displayed similar cylic voltammograms as with 0.8 L min^{-1}, but with a lower current density by three degrees of magnitude. We then suggest that the nanorod-like morphology increases the surface exposed to the electrolyte and consequently the value of the interchanged charge.

Inset of Figure 6 presents the discharge capacities of VO_2 (B) for the 1st and the 500th scan under a constant current density of 1 A g^{-1}. The chronopotentiometric curve presents one plateau, which indicates the one-step Li$^+$ intercalation process. The capacitance retention after 500 scans found to be 96 %, which is promising for practical applications in LIBs and supercapacitors. These outcomes can be further enhanced by the deposition of VO_2 on conducting flexible substrates that are expected to facilitate higher current densities.

4 Conclusions

Monoclinic and metastable VO_2 phases yield through the APCVD reaction of VO(acac)$_2$ on flexible glass substrates. It was possible to isolate these phases by controlling the oxygen flow rate through the reactor. The monoclinic VO_2 nanocrystallites show a reversible switching behavior at 62 ^{o}C with a difference in transmittance between the metallic and semiconducting phase of the order of 40 %. On the other hand, the hysteresis width found to be the largest compared with the others due to competing effects of crystallinity and crystallite size. Regarding the nanorod-like metastable VO_2 structures show good electrochemical response and discharge capacity, which are stable with minimal degradation for 500 scans. We believe that this relates to the increased surface area ratio of the particular morphology.

This route can then be cost-effective for applications in thermochromics, capacitors and LIBs with good performances if one considers its transfer in a roll-to-roll manufacturing process.

Acknowledgements

national funds (National Strategic Reference Framework 2007 - 2013).

References

[1] F. J. Morin, Phys. Rev. Lett., 1959, **3**, 34-36.

[2] J. B. Goodenough, J. Solid State Chem., 1971, **3**, 490-500.

[3] A. Cavalleri, T. Dekorsv, H. H. W. Chong, J. C. Kieffer, R. W. Schoenlein, Phys. Rev. B: Condens. Matter Mater. Phys., 2004, **70**, 161102-4.

[4] M. E. A. Warwick, R. Binions, J. Mater. Chem. A, 2014, **2**, 3275-3292.

[5] E. E. Chain, Appl. Opt., 1991, 30, 2782-2787.

[6] J. C. C. Fan, H. R. Fetterman, F. J. Bachner, P. M. Zavrasky, C. D. Parker, Appl. Phys. Lett., 1977, **31**, 11-13.

[7] I. Balberb, S. Trokman, J. Appl. Phys., 1975, **46**, 2111-2119.

[8] D. Louloudakis, D. Vernardou, E. Spanakis, N. Katsarakis, E. Koudoumas, Phys. Proc., 2013, **46**, 137-141.

[9] D. Vernardou, M. E. Pemble, D. W. Sheel, Chem. Vapor Depos, 2007, **13**, 158-162.

[10] D. Vernardou, M. E. Pemble, D. W. Sheel, Surf. Coat. Tech., 2004, **188-189**, 250-254.

[11] H. Q. Li, P. He, Y. G. Wang, E. Hosono, H. S. Zhou, J. Mater. Chem., 2011, **21**, 10999-11009.

[12] H. M. Liu, Y. G. Wang, K. X. Wang, E. Hosono, H. S. Zhou, J. Mater. Chem., 2009, **19**, 2835-2840.

[13] E. Baudrin, G. Sudant, D. Larcher, B. Dunn, J. M. Tarascon, Chem. Mater., 2006, **18**, 4369-4374.

[14] T. D. Manning, I. P. Parkin, R. J. H. Clark, D. Sheel, M. E. Pemble, D. Vernardou, J. Mater. Chem., 2002, **12**, 2936-2939.

[15] T. D. Manning, I. P. Parkin, Polyhedron, 2004, **23**, 3087-3095.

[16] T. Maruyama, Y. Ikuta, J. Mater. Sci., 1993, **28**, 5073-5078.

[17] D. Vernardou, M. E. Pemble, D. W. Sheel, Chem. Vapor Depos, 2006, **12**, 263-274.

[18] S. Mathur, T. Ruegamer, I. Grobelsek, Chem. Vapor Depos, 2007, **13**, 42-47.

[19] L. Kritikos, L. Zambelis, G. Papadimitropoulos, D. Davazoglou, Surf. Coat. Technol., 2007, **201**, 9334-9339.

[20] D. Vernardou, D. Louloudakis, E. Spanakis, N. Katsarakis, E. Koudoumas, Sol. Energ. Mat. Sol. C., 2014, **128**, 36-40.

[21] D. Vernardou, M. E. Pemble, D. W. Sheel, Thin Solid Films, 2008, **516**, 4502-4507.

[22] D. Vernardou, P. Paterakis, H. Drosos, E. Spanakis, I. M. Povey, M. E. Pemble, E. Koudoumas, N. Katsarakis, Sol. Energ. Mat. Sol. C., 2011, **95**, 2842-2847.

[23] D. Vernardou, D. Louloudakis, E. Spanakis, N. Katsarakis, E. Koudoumas, New J. Chem., 2014, **38**, 1959-1964.

[24] D. Vernardou, M. Apostolopoulou, D. Louloudakis, N. Katsarakis, E. Koudoumas, New J. Chem., 2014, **38**, 2098-2104.

[25] D. Vernardou, M. Apostolopoulou, D. Louloudakis, N. Katsarakis, E. Koudoumas, J. Colloid. Interf. Sci., 2014, **424**, 1-6.

[26] D. Vernardou, M. Apostolopoulou, D. Louloudakis, E. Spanakis, N. Katsarakis, E. Koudoumas, J. McGrath, M. E. Pemble, J. Alloy. Compd., 2014, **586**, 621-626.

[27] L. Dai, C. Cao, Y. Gao, H. Luo, Sol. Energ. Mat. Sol. C., 2011, **95**, 712-715.

[28] A. Awaluddin, M. E. Pemble, A. C. Jones, P. A. Willimas, J. Phys. IV, 2001, **11**, Pr3-531-Pr3-537.

[29] M. J. Crosbie, P. A. Lane, P. J. Wright, D. J. Williams, A. C. Jones, T. J. Leedham, C. L. Reeves, J. Jones, J. Cryst. Growth, 2000, **219**, 390-396.

[30] J. –C. Valmalette, J. –R. Gavarri, Mater. Sci. Eng. B., 1998, **54**, 168-173.

[31] I. P. Parkin, R. Binions, C. Piccirillo, C. S. Blackman, T. D. Manning, J. Nano Res., 2008, **2**, 1-20.

[32] M. Saeli, R. Binions, C. Piccirillo, G. Hyett, I. P. Parkin, Polyhedron, 2009, **28**, 2233-2239.

[33] F. Beleille, L. Mazerolles, J. Livage, Mater. Res. Bull., 1999, **34**, 2177-2184.

[34] R. Binions, C. Piccirillo, G. Hyett, I. P. Parkin, J. Mater. Chem., 2007, **17**, 4652-4660.

[35] C. H. Griffiths, H. K. Eastwood, J. Appl. Phys., 1974, **45**, 2201-2206.

[36] C. Blaauw, F. Leenhouts, F. Van der Woude, G. A. Sawatzky, J. Phys. C: Solid State Phys., 1975, **8**, 459-468.

[37] L. T. Kang, Y. F. Gao, Z. T. Zhang, J. Du, C. X. Cao, Z. Chen, H. J. Luo, J. Phys. Chem. C, 2010, **114**, 1901-1911.

[38] V. A. Klimov, I. O. Timofeeva, S. D. Khanin, E. B. Shadrin, A. V. Ilinskii, F. Silva-Andrade, Tech. Phys., 2002, **47**, 1134.

[39] I. A. Kharhaev, F. A. Chudnovskii, E. B. Shadri, Phys. Solid State, 1994, **36**, 898.

[40] R. Lopez, T. E. Haynes, L. A. Boatner, L. C. Feldman, R. F. Haglund Jr., Phys. Rev. B, 2002, **65**, 224113.

[41] J. Y. Suh, R. Lopez, L. C. Feldman, R. F. Haglund Jr., J. Appl. Phys., 2004, **96**, 1209-1213.

[42] D. Ruzmetov, S. D. Senanayake, V. Narayanamurti, S. Ramanathan, Phys. Rev. B, 2008, **77**, 195442-5.